On the Accuracy of Power Profile Estimation using MMSE or Deconvoluted Correlation-Based Profiles

Alix May, Fabien Boitier, Ana Ore Remigio, Patricia Layec
Nokia Bell Labs France, 12 rue Jean Bart, Massy, France
alix.may@nokia.com

Abstract: We evaluate the accuracy of the deconvolution of the longitudinal power profile computed using correlation-based method. We show that we obtain a similar accuracy to the MMSE approach in different cases. © 2024 The Author(s)

1. Introduction

Massive monitoring needs to be deployed to enable a marginless operation of optical networks as well as to identify failures and to construct digital twins. Monitoring methods using receiver-side digital signal processing received significant attention due to the ease of integration, wide coverage, and the non-necessity of deploying extra hardware. Specifically, several methods showed the estimation of the longitudinal power profile using a comparison between two signals, an emulated noise-free signal, and the received signal in which nonlinear effects have been accumulated. The methods can be split into two categories depending on the type of comparison: i) correlation-based method (CM) [1-4] and ii) minimum mean square error (MMSE) methods [5-6].

In [6], closed-form formulas are derived for both methods, and it is shown that the estimated power profile of CMs is a convolution of the true power profile and a spatial response function (SRF), explaining the observed poorer spatial resolution of CMs with respect to MMSE. In [7], the authors perform the deconvolution of the CM profile with the SRF using numerical simulations to increase its spatial resolution. Provided it gives accurate and robust results, performing deconvolution instead of MMSE removes the need to compute the inverse of a large matrix.

In this paper, we numerically assess the accuracy of longitudinal power profile using root-mean square error (RMSE) using either the deconvolution or the MMSE methods. We characterize their performance behavior with respect to different parameters such as the input power, the transmission distance, or the modulation format.

2. Principle of the deconvolution

To obtain the deconvoluted profile P_{deconv}, the correlation-based profile P_{corr} must be computed. For this, we use the modified CM [3], which is an adaptation of the original CM [1]. Using the notations used in [6], we can write how to obtain P_{corr} as a function of the chromatic dispersion operator $\widehat{D}_{z_1,z_2}$ from point z_1 to z_2 and the nonlinear operator $\widehat{N} = |\cdot|^2(\cdot)$:

$$P_{\mathrm{corr}}(z_k) = \rho_0\left(A_1[L,n], \widehat{D}_{z_k\,L}\,\widehat{N}\,\widehat{D}_{0\,z_k}\,A[0,n]\right) \tag{1}$$

where $\rho_m\left[A[n],B[m]\right] = E\left[A[n+m]B^*[n]\right]$ is the cross-correlation and $E[\cdot]$ is the expectation. $A[0,n]$ is the transmitted signal. $A_1[L,n] = A[L,n] - A_0[L,n]$ where $A[L,n]$ is the received signal after a transmission of L km and $A_0[L,n]$ is built by applying the total chromatic dispersion to $A[0,n]$. To obtain the full power profile, z_k is varied from 0 ($= z_0$) to L with spatial step size Δ_z. Now, the SRF must be calculated as the real part of the g(z) function [6]:

$$\mathrm{g}(\mathrm{z_j}) = \left[\widehat{D}^{-1}{}_{z_j\,0}\,\widehat{N}\,\widehat{D}_{z_j\,0}\,\rho_m\left[A[0,n],A[0,n]\right]\right]_{\mathrm{m=0}} \tag{2}$$

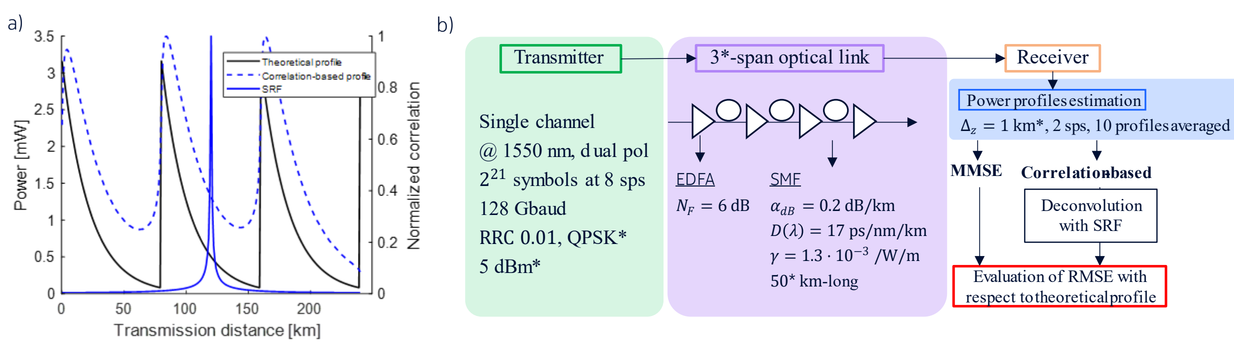

Figure 1: a) Theoretical and correlation-based profiles as well as the SRF in linear scale. b) Numerical set-up with default parameters. SMF: single-mode fiber. SRF: spatial response function. RRC: root-raised cosine. RMSE: root-mean square error. Parameters with * will be varied to determine their impact on the RMSE.

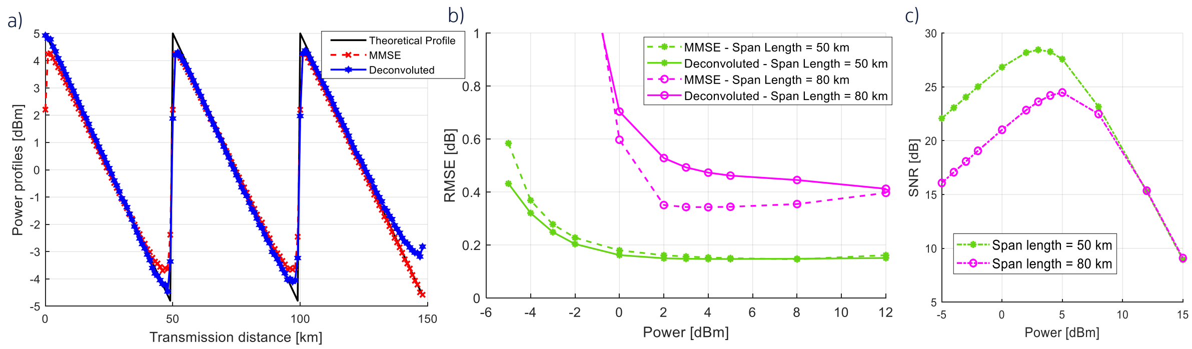

Figure 2: Results for QPSK 128 Gbaud 3-span transmission. a) Theoretical, MMSE and deconvoluted power profiles for 5 dBm. b) RMSE as a function of span input powers for MMSE and deconvoluted profiles for 50 and 80-km-long spans. c) Bell curve – SNR as a function of powers – for 50 and 80-km-long spans.

where z_j is varied from $-L/2$ to $+L/2$ with a spatial step Δ_z. Finally, the deconvoluted profile can be obtained as follows:

$$P_{\text{deconv}}(z_k) = \left[\mathrm{Re}(P_{\text{corr}}) \otimes_c F^{-1}\left(\frac{1}{F(Re(g))}\right)\right](z_k) \tag{3}$$

where $\otimes_c$ denotes the continuous spatial convolution, $F(\cdot)$ is the Fourier transform, $\mathrm{Re}(\cdot)$ the real part. We padded P_{corr} with zeros outside of the transmission link before applying the deconvolution filter. In Fig. 1a), we show a qualitative description of the deconvolution with the theoretical power, the correlation-based profile and the SRF.

3. Numerical set-up

To perform our evaluation, we use the numerical set-up described in Fig. 1b) where default parameters are written. Those with * may be varied in the following. A 128 Gbaud dual polarization quadrature phase shift keying (DP-QPSK) single channel with a roll-off factor of 0.01 is used. A digital predispersion of 200 km is applied to the transmitted signal. We consider an optical link with three 50-km-long spans. The output power of each erbium-doped fiber amplifier (EDFA) is 5 dBm. The noise figure of the EDFAs is set to 6 dB. The dispersion parameter of the emulated single-mode fibers (SMF) is 17 ps/nm/km. The nonlinear parameter is set to $1.3 \cdot 10^{-3}\ (\mathrm{W} \cdot \mathrm{m})^{-1}$. The attenuation value is set to 0.2 dB/km. We send 2^{21}-symbol sequences and the number of samples per symbol (sps) is set to 8 for the split-step-Fourier propagation. We calculate the SRF, the MMSE profile and the deconvoluted profile using fields at 2 sps. We use the formula in [Eq. (5),[5]] for the MMSE profile. To compare the accuracy of both methods, we compute the RMSE between the estimated profile and the theoretical power profile. Note that we excluded ± 3 km around EDFAs as well as the 10 first and last kms of transmission line to avoid any transition biases.

4. Results and discussion

We perform the deconvolution and using the default parameters described in Fig. 1b). In Fig. 2a), we show the obtained MMSE, deconvoluted as well as the theoretical power profiles. We see that, with those parameters, the deconvoluted power profile is very close to the MMSE profile, except at the end of the transmission line where it is further away. However, at the beginning of the line it is much closer to the theoretical one.

First, we evaluate the impact of the span input power. To this end, the power is varied from -5 to 12 dBm. We show in Fig. 2b) the RMSE as a function of powers for 50-km or 80-km -long spans. For 5 dBm and 50-km -long spans, we obtain a RMSE of 0.15 dB for deconvoluted and MMSE profiles. For all powers, we see that the RMSE are close for both methods. The RMSE continuously decreases when the power increases, due to the higher nonlinear effects, needed for power profile estimation. At -5 dBm, the RMSE is maximum and equals 0.43 dB (0.58 dB resp.) for the deconvoluted (MMSE, resp.) profile. An asymptote is reached when the power is larger than 1 dBm. Regarding the 80-km spans, the obtained RMSE are quite similar for MMSE and deconvoluted profiles, the difference with the 50-km span case being that the asymptote value is higher (~0.4 dB) due to the lower SNR and is reached for ~2 dBm. This study confirms the relevance and the robustness of the deconvolution to many input powers, including powers slightly lower than the nonlinear threshold (see Fig. 2c) showing the Bell curve).

Now, we investigate the impact of longer links, where we vary the number of 50-km -long spans from 3 to 24. We plot in Fig. 3a) the theoretical, MMSE and deconvoluted profiles when the number of spans is equal to 15. The deconvoluted profile is close to the MMSE one, except at the end of the spans specially for the beginning of the link. To validate this observation, in Fig. 3b), we plot the RMSE for both profiles versus the number of spans for two

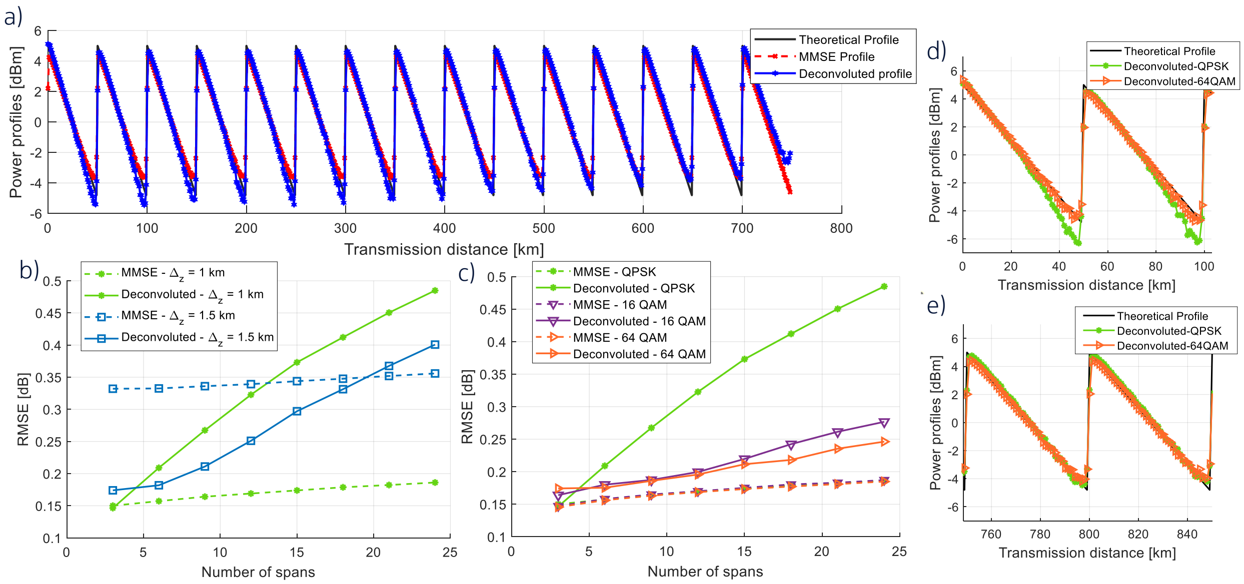

Figure 3: Results for 128 Gbaud 5 dBm. a) Theoretical, MMSE and deconvoluted power profiles for QPSK 15-span transmission with $\Delta_z = 1$ km. RMSE versus number of 50-km long spans for b) $\Delta_z = 1$ and 1.5 km and c) QPSK, 16 QAM and 64 QAM. Theoretical and deconvoluted profiles for 24 spans for QPSK and 64 QAM between d) 0 and 100 km and e) 750 and 850 km.

different spatial resolutions $\Delta_z = 1$ and 1.5 km. In all cases, the RMSE increases when the number of spans increases, due to the accumulation of noise. The MMSE method is more robust as the RMSE values do not vary much. However, we observe that while the deconvoluted profiles have a higher RMSE than the MMSE profiles for $\Delta_z = 1$ km, when $\Delta_z = 1.5$ km, the deconvoluted profiles have a smaller RMSE for up to 18 spans. This is due to the lower performance of MMSE when Δ_z is too large compared to the relatively high symbol rate to accurately model nonlinear effects. A larger Δ_z is interesting to accelerate computation speed.

Finally, we investigate the impact of the modulation format, knowing the CM is sensitive to it [6]. We plot in Fig. 3c) the RMSE for QPSK, 16-QAM and 64-QAM as a function of the number of spans. For all formats the RMSE increase when the number of spans increases. Note that the ‘deconvoluted – QPSK’ clearly stands out since the RMSE value equals 0.48 dB for 24 spans, while it is between 0.18 and 0.27 dB for all others. This is partly due to the poorer accuracy for the first spans at the end of them for QPSK compared to 16 and 64 QAM. We can see this effect in Fig. 3d) and e) where we focus on two subsets 0-100 and 750-850 km of the obtained deconvoluted profiles for the 24-span transmission for $\Delta_z = 1$ km. Compared to QPSK, with a higher modulation format, the accuracy of the deconvoluted profiles is improved and closer to the one of the MMSE for $\Delta_z = 1$ km for longer links.

5. Conclusion

In this article, we determined the accuracy of two power profile estimation methods: the deconvolution of CM and the MMSE method. We demonstrated that both methods show a similar accuracy for various powers and higher order modulation formats for $\Delta_z = 1$ km with a slight advantage for the MMSE method. We also showed the possibility to use both power profile estimation methods for longer links at the expense of a reasonable increase of the RMSE. For larger Δ_z, the deconvoluted profile can exhibit a better accuracy than MMSE profile.

This work was partly funded by EU Horizon 2020 B5G-OPEN Project (grant agreement 101016663).

6. References

[1] T. Tanimura *et al.*, “Fiber-Longitudinal Anomaly Position Identification Over Multi-Span Transmission Link Out of Receiver-end Signals,” in *Journal of Lightwave Technology*, May 2020, doi: 10.1109/JLT.2020.2984270.

[2] M. Sena *et al.*, “Advanced DSP-Based Monitoring for Spatially Resolved and Wavelength-Dependent Amplifier Gain Estimation and Fault Location in C+L-Band Systems,” in *Journal of Lightwave Technology*, Feb. 2023, doi: 10.1109/JLT.2022.3208209.

[3] C. Hahn *et al.*, "Localization of Reflection Induced Multi-Path-Interference Over Multi-Span Transmission Link by Receiver-side Digital Signal Processing," 2022 OFC, paper Th1C.3.

[4] A. May *et al.*, “Longitudinal Power Monitoring over a deployed 10,000-km Link for Submarine Systems,” 2023 OFC, Tu2G.3.

[5] T. Sasai, *et al.*, “0.77-dB anomaly loss localization based on DSP-Based fiber-longitudinal power estimation using linear least squares,” 2023 OFC, W1H.4.

[6] T. Sasai *et al.*, “Performance Limit of Fiber-Longitudinal Power Profile Estimation Methods,” in *Journal of Lightwave Technology*, vol. 41, no. 11, pp. 3278-3289, June 2023, doi: 10.1109/JLT.2023.3234534.

[7] C. Hahn *et al.*, "On the Spatial Resolution of Location-Resolved Performance Monitoring by Correlation Method," 2023 OFC, W1H.2.